García Núñez, C., Braña, A. F., López, N. and García, B. J. (2018) A novel growth method to improve the quality of GaAs nanowires grown by Ga-assisted chemical beam epitaxy. Nano Letters, 18(6), pp. 3608-3615.

There may be differences between this version and the published version. You are advised to consult the publisher's version if you wish to cite from it.

http://eprints.gla.ac.uk/162504/

Deposited on: 2 October 2018

Enlighten – Research publications by members of the University of Glasgow
http://eprints.gla.ac.uk

A Novel Growth Method to Improve the Quality of GaAs Nanowires Grown by Ga-Assisted Chemical Beam Epitaxy

*Carlos García Núñez,[†] Alejandro F. Braña, Nair López, Basilio J. García**

Electronics and Semiconductors Group (ELySE), Department of Applied Physics, Universidad Autónoma de Madrid, 28049 Madrid, Spain.

Keywords: GaAs Nanowires, Vapour-Solid-Liquid, Chemical Beam Epitaxy, Ga-assisted Growth, Nanowires Growth on Silicon, Vertically-aligned Nanowires

Abstract

The successful synthesis of high crystalline quality and high aspect ratio GaAs nanowires (NWs) with a uniform diameter is needed to develop advanced applications beyond the limits established by thin film and bulk material properties. Vertically aligned GaAs NWs have been extensively grown by Ga-assisted vapour-liquid-solid (VLS) mechanism on Si(111) substrates, and they have been used as building blocks in photovoltaics, optoelectronics, electronics, etc. However, the nucleation of parasitic species such as traces and nanocrystals on the Si substrate surface during the NW growth could affect significantly the controlled nucleation of those NWs, and therefore the resulting performance of NWs based devices. Preventing the nucleation of parasitic species on the Si substrate is a matter of interest, because they could act as traps for gaseous precursors and/or chemical elements during VLS growth, drastically reducing the maximum length of grown NWs, affecting their morphology and structure, and reducing the NW density along the Si substrate surface.

This work presents a novel and easy to develop growth method (i.e. without using advanced nano-lithography techniques) to prevent the nucleation of parasitic species, while preserving the quality of GaAs NWs even for long duration growths. GaAs NWs are grown by Ga-assisted chemical beam epitaxy on oxidized Si(111) substrates using triethylgallium and tertiarybutylarsine precursors by a two-steps based growth method presented here; this method includes a growth interruption for an oxidation on air between both steps of growth, reducing the nucleation of parasitic crystals on the thicker SiO_x capping layer during the second and longer growth step. VLS conditions are preserved overtime, resulting in a stable NW growth rate of around 6 μm/h for growth times up to 1 h. Resulting GaAs NWs have a high aspect ratio of 85 and average radius of

35 nm. We also report for the existence of characteristic reflection high-energy electron diffraction patterns associated to the epitaxial growth of GaAs NWs on Si(111) substrates, which have been analyzed and compared to the morphological characterization of GaAs NWs grown for different times under different conditions.

1. Introduction

Semiconductor nanowires (NWs) have demonstrated their validity and applicability as building blocks in advanced applications such as electronics, optoelectronics, photonics, photovoltaics and sensing,[1-6] overcoming functionalities and features achieved by thin film and bulk materials, due to their unique properties such as high surface-to-volume ratio, low dimensionality and high crystal quality (i.e. low defect density). Some examples in which GaAs NWs are expected to play a crucial role for the development of a wide number of high-performance applications include photovoltaic cells,[7] photodetectors,[8] resonant tunneling diodes,[9] single electron transistors,[10] and single photon emitters,[11] mainly based on their electronic transport properties, such as direct bandgaps and high carrier mobility. Currently available technology to integrate NWs on foreign substrates[6] or to develop electronic devices directly from as-grown NWs[12] presents still a poor performance; both approaches to develop NW-based electronic devices require a synthesis procedure capable to control the resulting density of NWs per unit area, NW aspect ratio (length to diameter ratio, L_{NW} / d_{NW}), NW morphology and NW crystal structure. The research on simple procedures to grow GaAs NWs with d_{NW} values below 100 nm and L_{NW} values above tenths of μm, while preserving their crystallinity and electronic/optoelectronic properties,

will allow for the development of high-performance electronic devices based on GaAs NWs, either directly grown on Si substrates or transferred to foreign substrates.

The growth of GaAs NWs through a bottom-up approach has been demonstrated by the well-known metal-assisted vapour-liquid-solid (VLS) mechanism, using a metallic particle to assist the growth of the NW along a preferential direction determined by the orientation of the crystalline substrate.[13] Vertically aligned GaAs NWs have been successfully grown on both Si(111) and GaAs(111)B substrates by different techniques, including molecular beam epitaxy (MBE)[14-21] and chemical beam epitaxy (CBE),[22-25] typically using Au and Ga as seed particles to form a supersaturated liquid alloy with growth species. Au has been extensively utilized in GaAs NW growths, but it could be incorporated as impurity into the NW structure,[26] and it could also induce zincblende/wurtzite (ZB/WZ) polytypisms along the NW body. These two important drawbacks support a wider use of Ga rather than Au for GaAs NW growth. Furthermore, theoretical models[27] that were experimentally confirmed,[24] have predicted and later demonstrated that Ga-assisted GaAs NWs present a better phase purity when Ga droplets partially wet the sidewalls of the NWs during the VLS based growth. However, the use of Si(111) with a thin capping oxide layer has shown the uncontrolled nucleation of other parasitic species, namely nanocrystals and traces, during Ga-assisted VLS growth of GaAs NWs by both MBE[28] and CBE[23-25] techniques, which could drastically affect some properties of resulting NWs. Pre-patterned SiO_x thick layers on both Si(111) and GaAs(111)B substrates have been extensively used to prevent the nucleation of parasitic species (Table 1).

The size uniformity obtained during Ga-assisted VLS growth of GaAs NWs has been recently analyzed as a function of precursor gas fluxes, in order to obtain highly uniform arrays of GaAs NWs on Si substrates.[17] Further investigations about the role of the Ga catalyst contact angle on

the resulting GaAs NW morphology have just demonstrated the possibility to grow high aspect-ratio GaAs NWs with d_{NW} below 20 nm, allowing the observation of quantum confinement effects.[15] All aforementioned achievements towards the accurate and reproducible growth of high quality GaAs NWs on Si substrates have been possible mainly due to the suitability of epitaxial techniques, including MBE and CBE, and to the study of different substrate pre-treatments. For the sake of comparison, Table 1 summarizes the performance obtained by different epitaxial techniques during the growth of vertically aligned GaAs NWs on Si(111) substrates by Ga-assisted VLS approach. This table also shows the pre-treatment of Si substrates prior to the growth to prevent the aforementioned parasitic species.

Table 1. Performance obtained from Ga-assisted VLS growths of GaAs NWs vertically aligned on either Si(111) or GaAs(111)B substrates, considering those approaches that successfully prevented the nucleation of parasitic species. The rows have been ordered as a function of the NW aspect ratio.

Technique	Substrate pre-treatment	NWs/μm^2	NW radius (nm)	NW aspect ratio	REF
MBE	e-beam lithography of nano-holes on 10-nm thick SiO_x/Si(111)	3	10	100	15
CBE	4-nm thick SiO_x/Si(111)	0.4	35	85	This Work
MBE	e-beam lithography of nano-holes on 15-nm thick SiO_x/GaAs(111)B	9	40	63	18
MBE	Nanoimprint lithography on 40-nm thick SiO_x/Si(111)	3	70	39	16
MBE	e-beam lithography of nano-holes on 10-nm thick SiO_x/Si(111)	8	80	33	17
MBE	e-beam lithography of nano-holes on 31-nm thick SiO_x/Si(111)	16	25	20	21
MBE	e-beam lithography of nano-holes on 31-nm thick SiO_x/Si(111)	15	30	17	14

As observed in Table 1, although the growth mechanisms of Ga-assisted GaAs NWs on Si(111) have been extensively analyzed as a function of growth conditions, only few studies have highlighted the nucleation of parasitic species and their role on the NW growth. Among all, advanced tools such as nano-lithography and high resolution photo-lithography have been successfully utilized to pattern nano-/micro-holes over a thick SiO_x surface layer on Si(111)

substrates, allowing the Ga-assisted VLS growth of GaAs NWs -mainly in MBE systems- to prevent parasitic species growth.[14,16] Additionally, those approaches permit a precise positioning of NWs along the substrate surface, controlling therefore the resulting NW density, which is critical for the development of electronic devices. However, lithographic procedures are not suitable for growth techniques using uncracked metalorganic precursors, such as CBE, since the growth on pre-patterned Si substrates requires a SiO_x layer with a thickness typically in the range of 20−30 nm, downgrading the cracking efficiency of metalorganic precursors on the substrate surface. The pre-patterning of nano-holes on SiO_x has been rarely used to grow a high density of uniform GaAs NWs over large areas (~2 inch wafer),[16] which is a feature required for applications such as large area photovoltaic cells. In this regard, the high-cost and incompatibility of techniques such as e-beam lithography to produce a massive number of nano-holes on SiO_x thick layers (i.e. nanometric hole-to-hole pitch), limit their applicability to grow well-ordered arrays of vertically aligned GaAs NWs over large areas.

In a previous work,[23] we have presented a thorough study on the growth mechanisms of GaAs NWs by Ga-assisted CBE on Si(111) substrates using triethylgallium (TEGa) and tertiarybuthylarsine (TBAs) as precursors, revealing the importance of the Si substrate surface preparation for the successful growth of NWs. In this work, we present an extended study on the NWs growth mechanism, introducing a novel method to preserve the growth conditions during long lasting VLS growths by hindering the formation of parasitic species, using neither nanolithography techniques nor complex substrate pre-treatments. Obtained NWs were analysed as a function of the growth conditions using scanning electron microscopy (SEM) to examine their morphology and density, and reflection high-energy electron diffraction (RHEED) to study their crystalline structure during the growth.

The results shown in this work are an important step forward to the optimization of the resulting quality of GaAs NWs grown on Si substrates, preventing the use of expensive tools and complex engineering procedures, and contributing to the development of higher performance electronic devices.

2. RESULTS AND DISCUSSION

2.1. One-step Growth Method

One- and two-steps based growth procedures developed in this work are schematically described in FIG 1, after an initial Si oxide layer was previously grown on top of the Si substrate. The one-step growth, having been thoroughly described elsewhere,[23] consists in: i) substrate thermal annealing for 5 min at a substrate temperature (T_s) of 650 ºC, in order to desorb remnant adsorbed molecules at the substrate surface (FIG 1(a)); ii) pre-deposition of TEGa equivalent to 7.5 Ga monolayers (MLs) at T_s = 580 ºC, allowing for Ga droplets formation on the oxidized Si(111) surface, followed by a stabilization stage for a time t_s = 90 s after TEGa valve is closed, leading to the rearrangement of Ga droplets on the substrate surface, and improving the resulting droplet size uniformity (FIG 1(b)); iii) finally, both TEGa and TBAs valves are opened at a V/III flux ratio of 0.8, starting the VLS growth of NWs at a growth rate (r_g) of around 5.4 μm/h (FIG 1(c)). The value of r_g has been estimated from the final nanowire length (L_{NW}) determined by SEM images after the growth time. NW growth was carried out under a substrate rotation of around 5 rpm to ensure a better gas flux uniformity on the substrate surface.

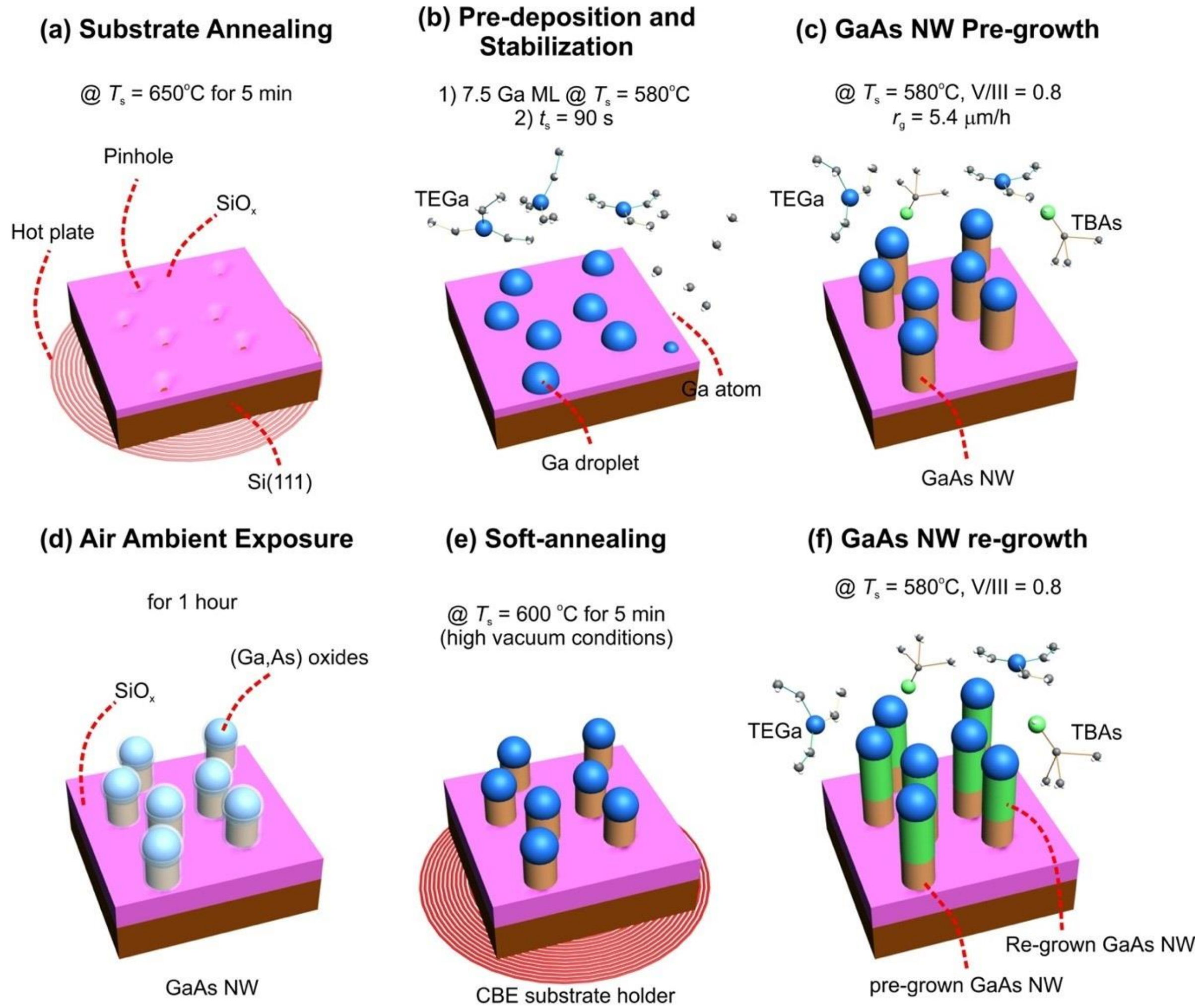

FIG 1. 3D Schematic illustration of the Ga-assisted CBE growth of GaAs NWs consisting in either (a-c) one-step or (a-f) two-steps based approaches. One-step approach consists of (a) Si(111) annealing at T_s = 650 ºC to create pinholes along the previously grown SiO_x thin surface layer; (b) TEGa pre-deposition at T_s = 580 ºC, resulting in Ga droplets randomly distributed along the substrate surface; (c) GaAs NW growth under TEGa and TBAs fluxes at T_s = 580 ºC. Two-steps approach comprises (d) air exposure of the sample grown in (a-c) to increase the SiO_x thickness; (e) soft-annealing at T_s = 600 ºC to desorb the oxide covering NWs and the Ga-catalyst; (f) re-growth of GaAs NWs using same conditions described in (c).

2.2. Two-steps Growth Method

The two-steps growth method starts with a GaAs NWs pre-growth carried out during 4 min under the same conditions than those previously described for the one-step growth method (FIG 1(a-c)). After this first step, the sample temperature is decreased to room temperature at the fastest allowed rate to reduce any residual growth as much as possible. After cooling down, the sample is taken out of the CBE system to be exposed to ambient air conditions for 1 hour to promote a controlled re-oxidation. This extra oxidation step increases the SiO_x thickness at those areas where NWs did not grow (FIG 1(d)). GaAs NWs and Ga droplets surfaces are also expected to be oxidized during this process. Thereafter, the samples are transferred again to the CBE system and annealed under ultra high vacuum for 5 min at T_s = 600 ºC. It is well known that native or chemical Ga and As oxide containing layers covering GaAs are usually desorbed at 580ºC prior to epitaxial growth, while Si oxide layers need much higher temperatures, in the 750-800 ºC range. The annealing temperature used here, T_s = 600 ºC, is expected to be high enough for desorption of Ga and As oxides covering NW sidewalls and Ga droplet, while it preserves Si oxide on the Si substrate surface (FIG 1(e)). It is worth noting that Si oxide thickness at this point is expected to be larger than the initial thickness before Ga droplet formation. Finally, T_s is lowered down to 580 ºC and a "re-growth" is carried out for different times by opening both TEGa and TBAs valves, using the same V/III flux ratio of 0.8 (FIG 1(f)).

2.3. Ga Droplet Nucleation on Si(111)

In a Ga-assisted growth, the formation of Ga droplets on top of the Si substrate surface is necessary to allow for the VLS growth of GaAs NWs.[23-25] Specially for CBE growth, the preparation of the Si(111) substrate prior to the growth process -i.e. the preparation of a thin film

of SiO_x- is crucial to enable the thermal decomposition of TEGa molecules on top of the oxidized Si surface, resulting in Ga droplets randomly distributed along the substrate surface (FIG 1(b)).[29] The chemical composition of the resultant Si(111) surface oxide after the application of etching protocols described above was analyzed by FTIR (see FIG S1(a)) and ATR (see FIG S1(b)). FTIR measurements show a diffuse reflectance signal with two main peaks centred around 1100 and 1250 cm^{-1} which are related to interstitial O (Si-O-Si) and stoichiometric SiO_2, respectively.[30] These results are in good agreement with previous works, where similar chemical treatments result in a SiO_x thin film with a random distribution of pinholes where Ga droplets can be preferentially formed.[29] The nucleation of Ga droplets on top of Si(111) substrates has been confirmed *in-situ* by RHEED and *ex-situ* by SEM elsewhere.[23] In those previous studies, we also analyzed Ga droplets size and their surface density as a function of Ga pre-deposition time and stabilization time, because they are crucial for controlling the distribution of NWs and their diameter.

2.4. One-step Growth Performance

During the NW growth, other GaAs features such as traces and nanocrystals (called here parasitic species) can also nucleate in the NWs vicinity (FIG 2(a,b)).[24,25] All tilted SEM images shown in this work, as FIG 2(b), were taken 30º away from the substrate surface normal direction. As this tilting value reduces the apparent vertical dimensions by a factor of sin 30º = 0.5, the real vertical scale has been multiplied by 2 in all tilted SEM images.

The nucleation of parasitic species was also observed in MBE processes using both thin[28] or thick dielectric layers,[29] and it has been linked to the chemical interaction between the Ga droplets and the dielectric layer. From FIG 2(a) one can conclude that there are two different collections of nanocrystals rotated 60º between each other, whose surfaces develop edges that are aligned with the hexagonal footprint of the NWs, indicating that nanocrystals have also nucleated on the Si

substrate in regions with a thinner or etched oxide. The density of parasitic species tends to increase over the growth time, which could be an important issue to preserve the initial growth conditions, thus limiting the maximum length of the NWs and hindering their aspect ratio. In this regard, we have previously reported[23] that GaAs NWs grown through a one-step method show an initially high r_g, while for growth times above 15 min a progressive reduction of r_g is observed, related to the nucleation of nanocrystalline GaAs. Nucleated GaAs nanocrystals increase their number and size as growth proceeds, until a layer covering the whole substrate surface is formed (see FIG S3), limiting the maximum achievable NW length to approximately 3 μm.

The formation of parasitic species was also confirmed by RHEED after 5−6 min of growth, when new spots in the diffraction pattern are observed, such as titled lines underneath the α and β lines and inter-spots labelled as δ in FIG 2(c). As the growth of parasitic species also consumes both Ga and As atoms, a reduction on the incorporation of these species to the droplet/NW interface will take place, altering the effective V/III ratio and decreasing the Ga droplet size. Since the NW diameter is affected by the size of the Ga droplet, its decrease also implies a reduction on the NW diameter, resulting in the tapering effect clearly observed in FIG 2(b). Furthermore, if the effective incorporation of Ga to the droplet is not sufficient, the droplet can be completely consumed by the VLS growth, finishing the longitudinal growth of the NWs when their length reaches about 3 μm. In addition to the above effect, the axial growth of the NW can be especially promoted at those regions near the NW base, which can be an additional factor contributing to the tapering effect observed in FIG 2(b). Another possible explanation for NWs tapering could be related to the change on the effective V/III ratio during NWs growth, due to the competition with parasitic species to incorporate Ga and As atoms.

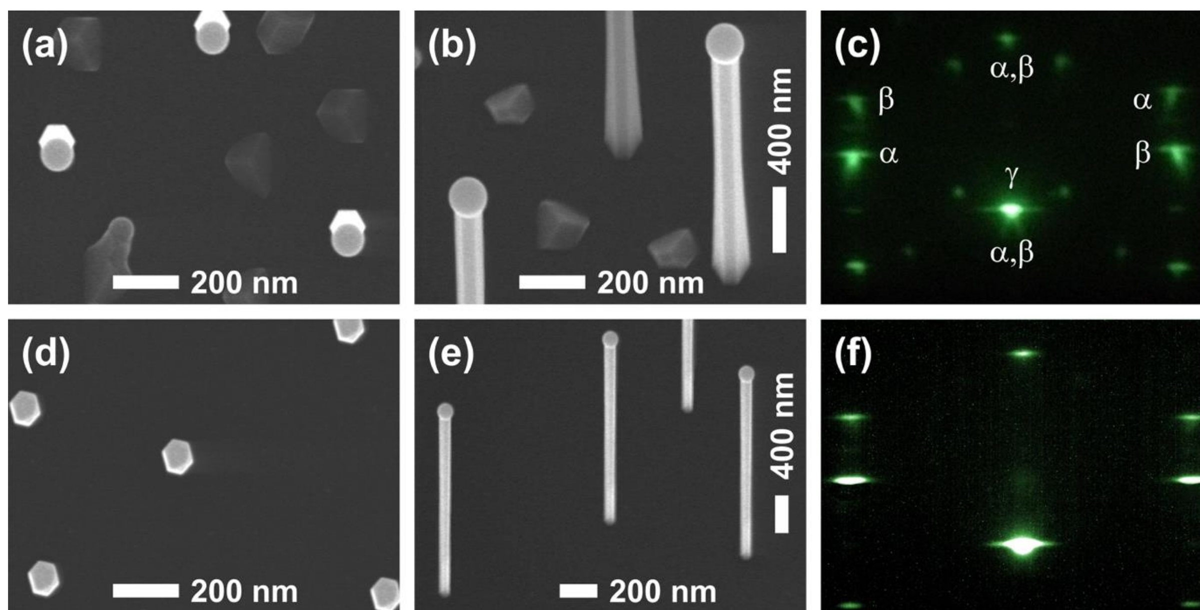

FIG 2. SEM images of GaAs NWs grown by (a,b) one-step and (d,e) two-steps growth methods taken at (a,d) 0º, and (b,e) 30º with respect to the substrate normal direction; (c) and (f) RHEED patterns corresponding to one-step and two-steps growth methods, respectively.

2.5. Two-steps Growth Performance

In the two-steps growth method, the scenario is very different from the one-step growth. The reduced 4 min growth time for the first growth step allows for the growth of short NWs (FIG 1(c)) while reducing the formation of parasitic species, whose growth rates are much slower, and their nucleation may be delayed. After the sample is exposed to the ambient air for 1 hour to increase the thickness of the SiO_x layer (FIG 1(d)), the small and thin parasitic structures, if any, that could have nucleated previously during the first growth step may also be fully oxidized, and allowed to be desorbed during the next annealing step.

After Ga and As oxide desorption, the re-growth step was then carried out using the same conditions than those used during pre-growth. FIG 2(d,e) show SEM images of resulting NWs,

observing a higher aspect ratio (L_{NW}/d_{NW} = 85, for 56-min re-growth time) and growth rates (r_g ~ 6 μm/h) than those obtained under the one-step growth method (L_{NW}/d_{NW} = 15 and r_g = 3 μm/h, respectively). This result can be explained on the basis of a drastic reduction of parasitic species under the two-steps growth method, which preserves the VLS conditions at the catalyst, allowing the growth of NWs with a better aspect ratio at a higher and constant growth rate, while observing no tapering effect (FIG 2 (d,e)).

From FIG 2(d,e) one can also conclude that the nucleation of parasitic species was totally inhibited by the two-steps growth procedure. FIG 2(f) presents the characteristic RHEED diffraction pattern under the <1-10> azimuth observed during the whole growth under the two-steps method; as mentioned before, horizontal lines correspond to NWs, whereas there was no evidence of inter-spots neither lines underneath the ZB lines, which confirms the absence of parasitic species. From above observations, RHEED has proved to be a precise tool to survey the formation of different species during NWs growth.

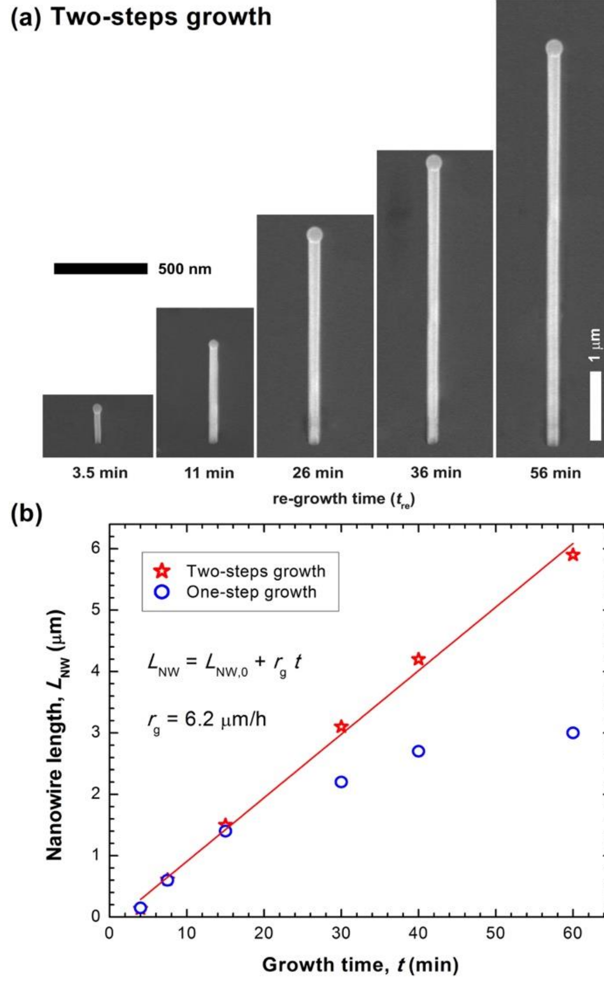

FIG 3. (a) SEM images of GaAs NWs grown under two-steps growth for different growth times; (b) NW length vs total growth time for GaAs NWs grown by one-step (blue circles) and two-steps (red starts) growth methods.

GaAs NWs were grown for different re-growth times (t_{re}) ranged between 3.5, 11, 26, 36, and 56 min after a pre-growth time (t_{pre}) of 4 min, resulting in a total growth time ($t = t_{pre} + t_{re}$) of 7.5, 15, 30, 40, and 60 min, respectively. Resulting NWs are shown in FIG 3(a), each NW image represents the average NW found for every sample, being representative of the observed NW population. FIG 3(b) represents the dependence of L_{NW} obtained from SEM images of GaAs NWs

grown under one-step (blue circles) and two-steps (red starts) growths, as a function of the growth time. In the two-steps growth procedure, L_{NW} exhibits a linear trend with the growth time, where r_g is around 6.2 μm/h. While both one-step and two-steps growth methods present approximately the same initial r_g value for growth times below 30 min, only the latter can preserve this stable r_g value, whereas r_g tends to decrease in the former, until the NW growth is stopped for growth times above 60 min.

The observed linear growth kinetics for NWs has also been reported by previous experimental works,[31-33] and it has also been predicted by using theoretical models.[34]

The promising result obtained through the two-steps growth method is accompanied by three more characteristics, namely the achievement of lower NW diameters, the observation of a drastic decrease -or even suppression- of parasitic species surrounding the NWs, and a high uniformity in density, size and height of NWs. These observations are clearly seen in FIG 4, which shows a wide field image of a sample with NWs grown during 15 min by the two-steps growth method, with an average density of 0.4 NW/μm^2.

Two-steps grown NWs described in this work have been successfully used to build a NW-based photodetector[35] by using NWs ultrasound lift-off in ethanol, followed by dielectrophoretic assembly of NWs on previously patterned contacts.

Summarizing, the best outcome obtained in our CBE system using the novel proposed two-steps growth method –included in Table 1– has shown a high density array of uniform and crystalline GaAs NWs vertically aligned on large area Si(111) substrates (~1 cm^2). SEM characterization of resulting samples shows an average NW density 0.4 NW/μm^2, with a homogeneous NW radius of 35 nm, and a uniform aspect ratio of 85, which are close to record values obtained using MBE.

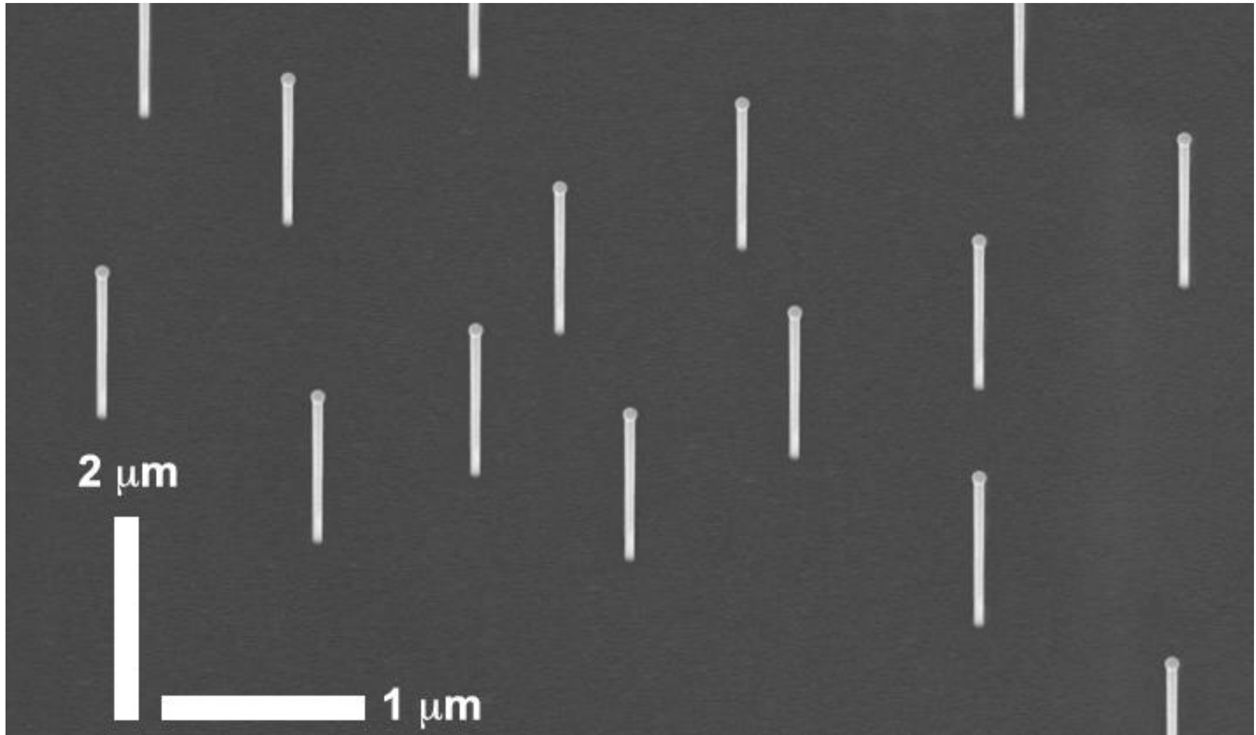

FIG 4. SEM image of GaAs NWs grown for 15 min on Si(111) by the described two-steps method.

3. CONCLUSIONS

We have developed a novel method to grow GaAs NWs by Ga-assisted CBE improving both NW aspect ratio (up to 85) and constant growth rate (~6.2 μm/h), obtaining NWs with lengths up to 6.2 μm and radius of 35 nm after a 1 hour growth. The proposed growth method is based on the growth of a thin SiO_x layer after a short pre-growth of GaAs NWs, and before a second and longer GaAs NW re-growth. This procedure has been demonstrated to reduce drastically the nucleation of parasitic GaAs nano-/micro-structures on the Si(111) substrate surface –as demonstrated *in-situ* by RHEED and *ex-situ* by SEM– and without the utilization of any complex and expensive tool such as nano-lithography. The simple approach proposed in this work favours the continuous and effective supply of Ga and As atoms to the growth interface formed between the NW and the Ga-catalyst, preserving VLS conditions and a nearly constant growth rate. As these are critical conditions required ~~in~~ for Ga-assisted VLS growth~~s~~ carried out in MBE and rarely achieved in CBE, our approach is promising for obtaining high-aspect ratio and high quality GaAs NWs on Si substrates.

4. MATERIALS AND METHODS

4.1. Growth system

GaAs NWs have been grown in a RIBER CBE32 system by Ga-assisted CBE on oxidized Si(111) substrates, using triethylgallium (TEGa) and tertiarybuthylarsine (TBAs) as Ga and As metalorganic precursors, respectively. TEGa and TBAs fluxes are controlled by a pressure regulated control system using an intermediate chamber for each precursor, located between each liquid container and the growth chamber and a calibrated hole. TBAs flux is directed to the substrate surface using a high temperature gas cracking cell (T_{HT} = 820 °C) to obtain reactive As-

containing species by pyrolysis, while uncracked TEGa flux is injected through a low temperature gas cell (T_{LT} = 80 ºC) to be dissociated on the substrate surface at the growth temperature T_s, ranged between 580 ºC < T_s < 620 ºC, which is measured by using a dual wavelength pyrometer.

4.2. Substrate Preparation

Samples used in this work consist in triangular-shaped cleaved pieces of Si(111) wafers (from Virginia Semiconductor), whose sides are limited by{-211} planes; the use of this kind of substrates allows for an easy identification of GaAs NW crystalline planes, relative to the Si substrate.

Prior to growth, substrates are etched in a 10% HF aqueous solution for 5 min and N_2 blow dried to remove the native oxide layer (SiO_x) capping the Si surface. The substrate surface after the above chemical etch is analyzed by means of Fourier transform infrared spectroscopy (FTIR), attenuated total reflectance (ATR) (see FIG S1(a,b)) and spectroscopic ellipsometry (SE) (see FIG S2). FTIR and ATR techniques are employed to study the chemical structure of SiO_x after the etching procedure, while SE is used to determine both residual oxide thickness and roughness. After etching, each substrate is In-bonded onto a molybdenum sample holder on a hot plate at 200 ºC. Once the substrate is cooled down to room temperature, it is etched again for 5 min by using the above HF solution, in order to remove the oxide grown during the bonding stage. Prior to introduction in the CBE system under high vacuum conditions, substrates are exposed to the ambient air conditions for 5 min to obtain the final SiO_x capping layer with a thickness of 1.5 nm, as determined by SE (see FIGS2), in a controlled way.

ASSOCIATED CONTENT

Supporting Information

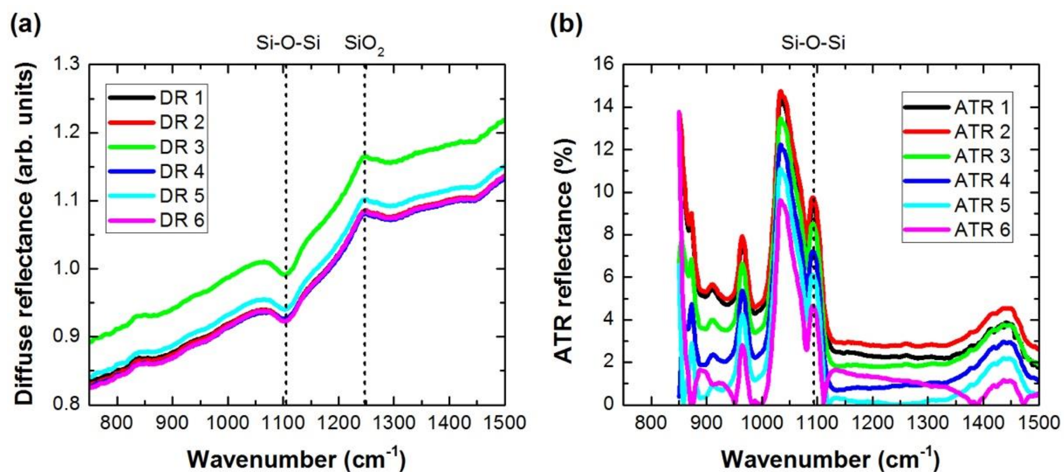

FIG S1. Fourier-transform infrared spectroscopy spectra of SiO_x for determination of oxide thickness on Si wafers.

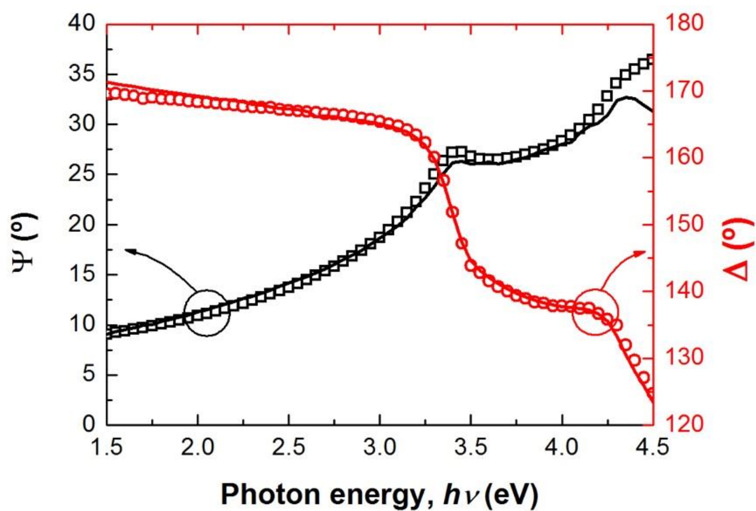

FIG S2. Spectroscopic ellipsometry measurements on a SiO_x/Si(111) sample after etching procedure (squares), and fitting a two-layer model (lines).

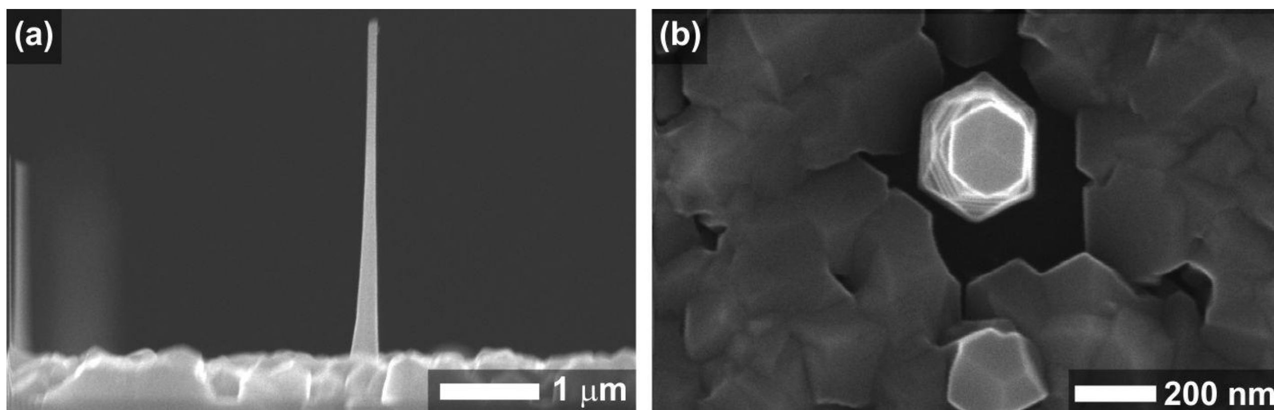

FIG S3. (a) cross-section and (b) top-view SEM images of a single GaAs NW grown under one-step growth conditions above 60 min.

AUTHOR INFORMATION

***Corresponding Author**

Prof. Basilio Javier García

Department of Applied Physics, Faculty of Sciences

Universidad Autónoma de Madrid

C/ Francisco Tomás y Valiente, 7, 28049 Madrid, Spain

e-mail: basilio.javier.garcia@uam.es

Present Addresses

†Micromanipulation Group, Electronics and Nanoscale Engineering, University of Glasgow, G128QQ Glasgow, United Kingdom.

Author Contributions

C.G.N. and B.J.G conceptualized the work; C.G.N. and B.J.G. carried out the synthesis and characterization of nanowires with support from A.F.B and N.L.; C.G.N. and B.J.G. wrote the manuscript with support from all co-authors; B.J.G. provided overall supervision for the project; All authors have given approval to the final version of the manuscript.

Funding Sources

Research work supported by the Spanish Ministerio de Ciencia e Innovación (TEC2010-20796).

Acknowledgment

This research was supported by the TEC2010-20796 (FPI grant), funded by the Spanish Ministerio de Ciencia e Innovación (MICINN). Authors are also thankful to the Servicio

Interdepartamental de Investigación (SIdI) at Universidad Autónoma de Madrid for technical support on the characterization of nanowires.

References

1. Lu, W.; Lieber, C. M., Semiconductor nanowires. *Journal of Physics D: Applied Physics* **2006,** *39* (21), R387.
2. Zhang, A.; Lieber, C. M., Nano-bioelectronics. *Chemical reviews* **2015,** *116* (1), 215-257.
3. Li, Y.; Qian, F.; Xiang, J.; Lieber, C. M., Nanowire electronic and optoelectronic devices. *Materials today* **2006,** *9* (10), 18-27.
4. Tian, B.; Kempa, T. J.; Lieber, C. M., Single nanowire photovoltaics. *Chemical Society Reviews* **2009,** *38* (1), 16-24.
5. Heiss, M.; Fontana, Y.; Gustafsson, A.; Wüst, G.; Magen, C.; O'regan, D.; Luo, J.; Ketterer, B.; Conesa-Boj, S.; Kuhlmann, A., Self-assembled quantum dots in a nanowire system for quantum photonics. *Nature materials* **2013,** *12* (5), 439.
6. García Núñez, C.; García Marín, A.; Nanterne, P.; Piqueras, J.; Kung, P.; Pau, J. L., Conducting Properties of Nearly Depleted ZnO Nanowire UV Sensors Fabricated by Dielectrophoresis. *Nanotechnology* **2013,** *24* (41), 415702.
7. Krogstrup, P.; Jørgensen, H. I.; Heiss, M.; Demichel, O.; Holm, J. V.; Aagesen, M.; Nygard, J.; i Morral, A. F., Single-nanowire solar cells beyond the Shockley-Queisser limit. *Nature Photonics* **2013,** *7* (4), 306-310.
8. Wang, H., High gain single GaAs nanowire photodetector. *Applied Physics Letters* **2013,** *103* (9), 093101.
9. Björk, M.; Ohlsson, B.; Thelander, C.; Persson, A.; Deppert, K.; Wallenberg, L.; Samuelson, L., Nanowire resonant tunneling diodes. *Applied Physics Letters* **2002,** *81* (23), 4458-4460.
10. Kasai, S.; Hasegawa, H., A single electron binary-decision-diagram quantum logic circuit based on Schottky wrap gate control of a GaAs nanowire hexagon. *Electron Device Letters, IEEE* **2002,** *23* (8), 446-448.
11. Heinrich, J.; Huggenberger, A.; Heindel, T.; Reitzenstein, S.; Höfling, S.; Worschech, L.; Forchel, A., Single photon emission from positioned GaAs/AlGaAs photonic nanowires. *Applied Physics Letters* **2010,** *96* (21), 211117.
12. Tang, Y.; Chen, Z.; Song, H.; Lee, C.; Cong, H.; Cheng, H.; Zhang, W.; Bello, I.; Lee, S., Vertically aligned p-type single-crystalline GaN nanorod arrays on n-type Si for heterojunction photovoltaic cells. *Nano letters* **2008,** *8* (12), 4191-4195.
13. Wagner, R. S.; Ellis, W. C., VAPOR-LIQUID-SOLID MECHANISM OF SINGLE CRYSTAL GROWTH. *Applied Physics Letters* **1964,** *4* (5), 89-90.
14. Plissard, S.; Larrieu, G.; Wallart, X.; Caroff, P., High yield of self-catalyzed GaAs nanowire arrays grown on silicon via gallium droplet positioning. *Nanotechnology* **2011,** *22* (27), 275602.
15. Kim, W.; Dubrovskii, V. G.; Vukajlovic-Plestina, J.; Tütüncüoglu, G.; Francaviglia, L.; Güniat, L.; Potts, H.; Friedl, M.; Leran, J.-B.; Fontcuberta i Morral, A., Bi-stability of contact angle and its role in achieving quantum-thin self-assisted GaAs nanowires. *Nano letters* **2018**.
16. Munshi, A. M.; Dheeraj, D. L.; Fauske, V. T.; Kim, D.-C.; Huh, J.; Reinertsen, J. F.; Ahtapodov, L.; Lee, K.; Heidari, B.; Van Helvoort, A., Position-controlled uniform GaAs nanowires on silicon using nanoimprint lithography. *Nano letters* **2014,** *14* (2), 960-966.
17. Vukajlovic-Plestina, J.; Kim, W.; Dubrovski, V. G.; Tütüncüoğlu, G.; Lagier, M.; Potts, H.; Friedl, M.; Fontcuberta i Morral, A., Engineering the Size Distributions of Ordered GaAs Nanowires on Silicon. *Nano Letters* **2017,** *17* (7), 4101-4108.

18. Bauer, B.; Rudolph, A.; Soda, M.; i Morral, A. F.; Zweck, J.; Schuh, D.; Reiger, E., Position controlled self-catalyzed growth of GaAs nanowires by molecular beam epitaxy. *Nanotechnology* **2010,** *21* (43), 435601.
19. Russo-Averchi, E.; Vukajlovic Plestina, J.; Tütüncüoglu, G.; Matteini, F.; Dalmau-Mallorquí, A.; de la Mata, M.; Rüffer, D.; Potts, H. A.; Arbiol, J.; Conesa-Boj, S.; Fontcuberta i Morral, A., High Yield of GaAs Nanowire Arrays on Si Mediated by the Pinning and Contact Angle of Ga. *Nano Letters* **2015,** *15* (5), 2869-2874.
20. Gibson, S.; LaPierre, R., Study of radial growth in patterned self-catalyzed GaAs nanowire arrays by gas source molecular beam epitaxy. *physica status solidi (RRL) – Rapid Research Letters* **2013,** *7* (10), 845-849.
21. Dubrovskii, V.; Xu, T.; Álvarez, A. D.; Plissard, S.; Caroff, P.; Glas, F.; Grandidier, B., Self-equilibration of the diameter of Ga-catalyzed GaAs nanowires. *Nano letters* **2015,** *15* (8), 5580-5584.
22. Persson, A.; Ohlsson, B.; Jeppesen, S.; Samuelson, L., Growth mechanisms for GaAs nanowires grown in CBE. *Journal of crystal growth* **2004,** *272* (1), 167-174.
23. García Núñez, C.; Braña, A. F.; López, N.; García, B. J., GaAs nanowires grown by Ga-assisted chemical beam epitaxy: Substrate preparation and growth kinetics. *J. Cryst. Growth* **2015,** *430*, 108-115.
24. García Núñez, C.; Braña, A. F.; Pau, J. L.; Ghita, D.; García, B. J.; Shen, G.; Wilbert, D. S.; Kim, S. M.; Kung, P., Pure zincblende GaAs nanowires grown by Ga-assisted chemical beam epitaxy. *Journal of Crystal Growth* **2013,** *372*, 205-212.
25. García Núñez, C.; Braña, A. F.; Pau, J. L.; Ghita, D.; García, B. J.; Shen, G.; Wilbert, D. S.; Kim, S. M.; Kung, P., Surface optical phonons in GaAs nanowires grown by Ga-assisted chemical beam epitaxy. *Journal of Applied Physics* **2014,** *115* (3), 034307.
26. Perea, D. E.; Allen, J. E.; May, S. J.; Wessels, B. W.; Seidman, D. N.; Lauhon, L. J., Three-dimensional nanoscale composition mapping of semiconductor nanowires. *Nano letters* **2006,** *6* (2), 181-185.
27. Dubrovskii, V.; Cirlin, G.; Sibirev, N.; Jabeen, F.; Harmand, J.; Werner, P., New mode of vapor− liquid− solid nanowire growth. *Nano letters* **2011,** *11* (3), 1247-1253.
28. Matteini, F.; Dubrovskii, V. G.; Rüffer, D.; Tütüncüoğlu, G.; Fontana, Y.; Morral, A. F. I., Tailoring the diameter and density of self-catalyzed GaAs nanowires on silicon. *Nanotechnology* **2015,** *26* (10), 105603.
29. Fontcuberta i Morral, A.; Colombo, C.; Abstreiter, G.; Arbiol, J.; Morante, J., Nucleation mechanism of gallium-assisted molecular beam epitaxy growth of gallium arsenide nanowires. *Applied Physics Letters* **2008,** *92* (6), 063112-063112-3.
30. Matteini, F.; Tutuncuoglu, G.; Rüffer, D.; Alarcon-Llado, E.; Morral, A., Untangling the role of oxide in Ga-assisted growth of GaAs nanowires on Si substrates. *arXiv preprint arXiv:1307.6113* **2013**.
1. Lu, W.; Lieber, C. M., Semiconductor nanowires. *Journal of Physics D: Applied Physics* **2006,** *39* (21), R387.
2. Zhang, A.; Lieber, C. M., Nano-bioelectronics. *Chemical reviews* **2015,** *116* (1), 215-257.
3. Li, Y.; Qian, F.; Xiang, J.; Lieber, C. M., Nanowire electronic and optoelectronic devices. *Materials today* **2006,** *9* (10), 18-27.
4. Tian, B.; Kempa, T. J.; Lieber, C. M., Single nanowire photovoltaics. *Chemical Society Reviews* **2009,** *38* (1), 16-24.

5. Heiss, M.; Fontana, Y.; Gustafsson, A.; Wüst, G.; Magen, C.; O'regan, D.; Luo, J.; Ketterer, B.; Conesa-Boj, S.; Kuhlmann, A., Self-assembled quantum dots in a nanowire system for quantum photonics. *Nature materials* **2013,** *12* (5), 439.
6. García Núñez, C.; García Marín, A.; Nanterne, P.; Piqueras, J.; Kung, P.; Pau, J. L., Conducting Properties of Nearly Depleted ZnO Nanowire UV Sensors Fabricated by Dielectrophoresis. *Nanotechnology* **2013,** *24* (41), 415702.
7. Krogstrup, P.; Jørgensen, H. I.; Heiss, M.; Demichel, O.; Holm, J. V.; Aagesen, M.; Nygard, J.; i Morral, A. F., Single-nanowire solar cells beyond the Shockley-Queisser limit. *Nature Photonics* **2013,** *7* (4), 306-310.
8. Wang, H., High gain single GaAs nanowire photodetector. *Applied Physics Letters* **2013,** *103* (9), 093101.
9. Björk, M.; Ohlsson, B.; Thelander, C.; Persson, A.; Deppert, K.; Wallenberg, L.; Samuelson, L., Nanowire resonant tunneling diodes. *Applied Physics Letters* **2002,** *81* (23), 4458-4460.
10. Kasai, S.; Hasegawa, H., A single electron binary-decision-diagram quantum logic circuit based on Schottky wrap gate control of a GaAs nanowire hexagon. *Electron Device Letters, IEEE* **2002,** *23* (8), 446-448.
11. Heinrich, J.; Huggenberger, A.; Heindel, T.; Reitzenstein, S.; Höfling, S.; Worschech, L.; Forchel, A., Single photon emission from positioned GaAs/AlGaAs photonic nanowires. *Applied Physics Letters* **2010,** *96* (21), 211117.
12. Tang, Y.; Chen, Z.; Song, H.; Lee, C.; Cong, H.; Cheng, H.; Zhang, W.; Bello, I.; Lee, S., Vertically aligned p-type single-crystalline GaN nanorod arrays on n-type Si for heterojunction photovoltaic cells. *Nano letters* **2008,** *8* (12), 4191-4195.
13. Wagner, R. S.; Ellis, W. C., VAPOR-LIQUID-SOLID MECHANISM OF SINGLE CRYSTAL GROWTH. *Applied Physics Letters* **1964,** *4* (5), 89-90.
14. Plissard, S.; Larrieu, G.; Wallart, X.; Caroff, P., High yield of self-catalyzed GaAs nanowire arrays grown on silicon via gallium droplet positioning. *Nanotechnology* **2011,** *22* (27), 275602.
15. Kim, W.; Dubrovskii, V. G.; Vukajlovic-Plestina, J.; Tütüncüoglu, G.; Francaviglia, L.; Güniat, L.; Potts, H.; Friedl, M.; Leran, J.-B.; Fontcuberta i Morral, A., Bi-stability of contact angle and its role in achieving quantum-thin self-assisted GaAs nanowires. *Nano letters* **2018**.
16. Munshi, A. M.; Dheeraj, D. L.; Fauske, V. T.; Kim, D.-C.; Huh, J.; Reinertsen, J. F.; Ahtapodov, L.; Lee, K.; Heidari, B.; Van Helvoort, A., Position-controlled uniform GaAs nanowires on silicon using nanoimprint lithography. *Nano letters* **2014,** *14* (2), 960-966.
17. Vukajlovic-Plestina, J.; Kim, W.; Dubrovski, V. G.; Tütüncüoğlu, G.; Lagier, M.; Potts, H.; Friedl, M.; Fontcuberta i Morral, A., Engineering the Size Distributions of Ordered GaAs Nanowires on Silicon. *Nano Letters* **2017,** *17* (7), 4101-4108.
18. Bauer, B.; Rudolph, A.; Soda, M.; i Morral, A. F.; Zweck, J.; Schuh, D.; Reiger, E., Position controlled self-catalyzed growth of GaAs nanowires by molecular beam epitaxy. *Nanotechnology* **2010,** *21* (43), 435601.
19. Russo-Averchi, E.; Vukajlovic Plestina, J.; Tütüncüoglu, G.; Matteini, F.; Dalmau-Mallorquí, A.; de la Mata, M.; Rüffer, D.; Potts, H. A.; Arbiol, J.; Conesa-Boj, S.; Fontcuberta i Morral, A., High Yield of GaAs Nanowire Arrays on Si Mediated by the Pinning and Contact Angle of Ga. *Nano Letters* **2015,** *15* (5), 2869-2874.

20. Gibson, S.; LaPierre, R., Study of radial growth in patterned self-catalyzed GaAs nanowire arrays by gas source molecular beam epitaxy. *physica status solidi (RRL) – Rapid Research Letters* **2013,** *7* (10), 845-849.
21. Dubrovskii, V.; Xu, T.; Álvarez, A. D.; Plissard, S.; Caroff, P.; Glas, F.; Grandidier, B., Self-equilibration of the diameter of Ga-catalyzed GaAs nanowires. *Nano letters* **2015,** *15* (8), 5580-5584.
22. Persson, A.; Ohlsson, B.; Jeppesen, S.; Samuelson, L., Growth mechanisms for GaAs nanowires grown in CBE. *J. Cryst. Growth* **2004,** *272* (1), 167-174.
23. García Núñez, C.; Braña, A. F.; López, N.; García, B. J., GaAs Nanowires Grown by Ga-assisted Chemical Beam Epitaxy: Substrate Preparation and Growth Kinetics. *J. Cryst. Growth* **2015,** *430*, 108-115.
24. García Núñez, C.; Braña, A. F.; Pau, J. L.; Ghita, D.; García, B. J.; Shen, G.; Wilbert, D. S.; Kim, S. M.; Kung, P., Pure zincblende GaAs nanowires grown by Ga-assisted chemical beam epitaxy. *Journal of Crystal Growth* **2013,** *372*, 205-212.
25. García Núñez, C.; Braña, A. F.; Pau, J. L.; Ghita, D.; García, B. J.; Shen, G.; Wilbert, D. S.; Kim, S. M.; Kung, P., Surface optical phonons in GaAs nanowires grown by Ga-assisted chemical beam epitaxy. *Journal of Applied Physics* **2014,** *115* (3), 034307.
26. Perea, D. E.; Allen, J. E.; May, S. J.; Wessels, B. W.; Seidman, D. N.; Lauhon, L. J., Three-dimensional nanoscale composition mapping of semiconductor nanowires. *Nano letters* **2006,** *6* (2), 181-185.
27. Dubrovskii, V.; Cirlin, G.; Sibirev, N.; Jabeen, F.; Harmand, J.; Werner, P., New mode of vapor− liquid− solid nanowire growth. *Nano letters* **2011,** *11* (3), 1247-1253.
28. Matteini, F.; Dubrovskii, V. G.; Rüffer, D.; Tütüncüoğlu, G.; Fontana, Y.; Morral, A. F. I., Tailoring the diameter and density of self-catalyzed GaAs nanowires on silicon. *Nanotechnology* **2015,** *26* (10), 105603.
29. Fontcuberta i Morral, A.; Colombo, C.; Abstreiter, G.; Arbiol, J.; Morante, J., Nucleation mechanism of gallium-assisted molecular beam epitaxy growth of gallium arsenide nanowires. *Applied Physics Letters* **2008,** *92* (6), 063112-063112-3.
30. Matteini, F.; Tutuncuoglu, G.; Rüffer, D.; Alarcon-Llado, E.; Morral, A., Untangling the role of oxide in Ga-assisted growth of GaAs nanowires on Si substrates. *arXiv preprint arXiv:1307.6113* **2013**.
31. Colombo, C.; Spirkoska, D.; Frimmer, M.; Abstreiter, G.; i Morral, A. F., Ga-assisted catalyst-free growth mechanism of GaAs nanowires by molecular beam epitaxy. *Physical Review B* **2008,** *77* (15), 155326.
32. Dayeh, S. A.; Soci, C.; Bao, X.-Y.; Wang, D., Advances in the synthesis of InAs and GaAs nanowires for electronic applications. *Nano Today* **2009,** *4* (4), 347-358.
33. Jensen, L. E.; Björk, M. T.; Jeppesen, S.; Persson, A. I.; Ohlsson, B. J.; Samuelson, L., Role of surface diffusion in chemical beam epitaxy of InAs nanowires. *Nano Letters* **2004,** *4* (10), 1961-1964.
34. Dubrovskii, V.; Sibirev, N.; Cirlin, G.; Soshnikov, I.; Chen, W.; Larde, R.; Cadel, E.; Pareige, P.; Xu, T.; Grandidier, B., Gibbs-Thomson and diffusion-induced contributions to the growth rate of Si, InP, and GaAs nanowires. *Physical Review B* **2009,** *79* (20), 205316.
35. García Núñez, C.; Braña, A. F.; López, N.; Pau, J. L.; García, B. J. In *Photodetector fabrication by dielectrophoretic assembly of GaAs nanowires grown by a two-steps method*, SPIE Nanoscience + Engineering, San Diego, SPIE: San Diego, 2017; p 103530F.

TOC Figure